Stellar Spectroscopy - Astro02

James R. McMurray
Demonstrator: Dr. Jennifer Hatchell
(Dated: March 27, 2011)

In this investigation spectra were obtained from Mars, the Moon, Sirius, Betelgeuse and the daytime sky. The spectra of the daytime sky and the Moon appeared much redder than they should have, and the exact cause of this is unknown. The effective surface temperatures of the stars were then calculated using Wien's Law, the temperature of Sirius was calculated to be 7149 ± 200K while the accepted value is 9940K[1], and the effective surface temperature of Betelgeuse was calculated to be 3838 ± 200K which is not consistent with the accepted value of 3500K.

INTRODUCTION

In this investigation, spectra were obtained from the stars, Sirius and Betelgeuse, Mars, the Moon and the daytime sky, so that spectra of different types could be compared. The spectra were analysed, the major peaks were identified and the equivalent widths measured. The temperatures were then estimated by the peaks of the spectra, and other possibilities and difficulties discussed.

THEORY

Continuous Spectra

Stars emit a continuous spectrum of light which can be modelled as a blackbody emitter. The equation for this radiation distribution is given in Equation (1), in terms of wavelength[2].

$$I_\lambda(\lambda, T_s) = \frac{2hc^2}{\lambda^5} \frac{1}{\exp(hc/\lambda k T_s) - 1} \tag{1}$$

Where I_λ is the power emitted per unit wavelength per unit area per unit solid angle, λ is the wavelength, T_s is the effective surface temperature, h is Planck's constant, c is the speed of light in a vacuum and k is Boltzmann's constant. A diagram showing example plots of blackbody distributions at different temperatures is given in Figure 1.

The effective surface temperature can be calculated from the continuous spectrum from Wien's Law given in Equation (2).

$$T_s \lambda_{\text{peak}} = b \tag{2}$$

where T_s is the effective surface temperature, λ_{peak} is the peak wavelength and b is a constant termed Wien's displacement constant[3].

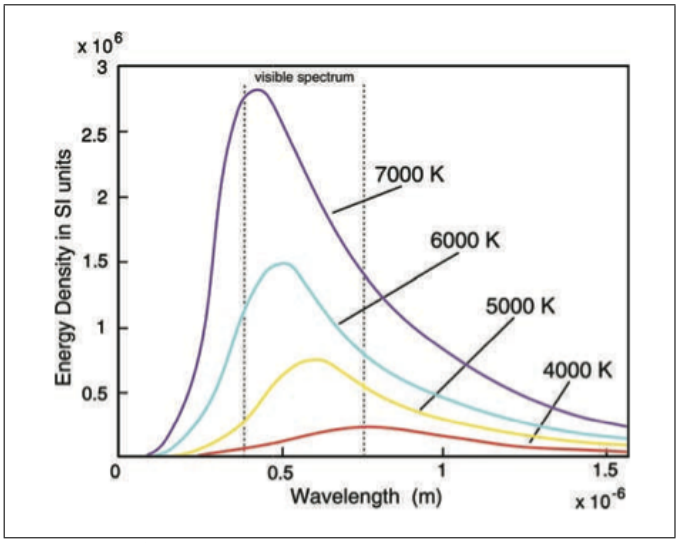

FIG. 1: A diagram showing black body distributions at various temperatures. Adapted from [1].

Absorption Lines

However, there are also characteristic absorption lines in the spectrum which mean it is not entirely described by the black-body distribution. These absorption lines are black lines in the spectrum from the absorption of the emitted light at specific frequencies by the elements in the star. These absorption lines are specific to certain elements (they match the stimulated emission frequencies) and so can be used to determine the chemical composition of stars.

However, the chemical composition of stars is very similar (approximately 72% Hydrogen, 25% Helium and 3% metals) and so the chemical composition is not main source of the difference between spectra. The main factor producing the variety of absorption lines and sizes is the variation in stellar temperature which results in differences in the level of ionisation and the relative atomic populations.

The lines can be identified from a known list of Fraunhofer lines, named after Joseph von Fraunhofer who first observed spectral lines in 1814[4].

The strength of spectral lines can be represented by

the equivalent width, which is the width that a rectangle would have with the same area as the absorption line and the same flux as the level of the continuous radiation at that point. The strength of the absorption line is a measure of the relative abundance of the species responsible for the absorption line.

Specifically the Balmer series of hydrogen (the stimulated emission peaks from transitions to the second energy level of the atom) is significant in the visible range of the spectrum, as the different populations of the atoms responsible for the different lines vary significantly with temperature, and so the ratios of the peaks can be used to determine the surface temperature of the star. For as the surface temperature of the star increases, the hydrogen atoms are ionised and so cannot produce absorption lines as there are no electrons available for possible transitions, this means that the absorption peaks are weaker in hotter stars[3]. The lines are most prominent when the star is hot enough to excite the electron out of the ground state but not so hot as to produce ionisation.

The wavelengths of the Balmer series are given by Equation (3).

$$\lambda = B\left(\frac{m^2}{m^2-4}\right) \tag{3}$$

Where λ is the wavelength of the line, B is the Balmer constant with a value of 3.6456×10^{-7} m and m is an integer above 2.

The absorption peaks are also effected by the Doppler shift, the magnitude and direction of the shift can be used to calculate the relative radial velocity of the stars (assuming the observer to be stationary). The non-relativistic Doppler shift equation is given in Equation (4) in terms of frequency.

$$f = \left(\frac{c}{c+v_{\text{rel}}}\right) f_0 \tag{4}$$

Where f os the observed frequency of the peaks, c is the speed of light (the speed of the wave), v_{rel} is the relative radial velocity of the star and f_0 is the position of the peak when stationary (i.e. measured from an emission lamp on Earth).

The ratio of the lines can be used to classify the stars by spectral type and luminosity class.

Peak Broadening

The absorption peaks do not simply appear as lines in the spectra due to the phenomenon of peak broadening. Peak broadening has a variety of sources. The most fundamental source of broadening is the natural linewidth set by the Heisenberg Uncertainty principle, as there must be a minimum uncertainty in the frequency (and so the wavelength) of the absorption, however this effect is very small (on the order of 10^{-4} Å).

Other sources of broadening include temperature broadening, where the random movement of the gas molecules due to their temperature creates small Doppler shifts in the absorbed frequencies and so results in broadening. Rotational broadening is the broadening of the peaks due to the rotation of the stars creating small Doppler shifts in the peaks (dependent on the speed of rotation).

High pressure can also produce broadening through the Stark effect, as the external electric field causes the energy levels to shift and split.

Note that the thermal and rotational broadening (Doppler broadening) results in broadening to a Gaussian profile whereas the natural linewidth and pressure broadening results in a broadening to a Lorentzian profile. When these are combined the broadening fits a combination called a Voigt profile.

Stellar Classification

Stars are classified according to their temperature by their spectral types, and their luminosity by their luminosity class.

Spectral Type

Stars are assigned a spectral type according to their temperature, in order of decreasing temperature these are: O, B, A, F, G, K and M. There are also additional spectral types for Wolf-Rayet stars, red and brown dwarfs and carbon stars.

The types themselves are subdivided in to ten spectral classes from 0 to 9 in order of decreasing temperature, so a class A1 star is hotter than a class A8 star which is in turn hotter than a class F0 star[3].

Luminosity class

The stars are also assigned a luminosity class, in order of decreasing luminosity these are[3]:

I Supergiants

II Bright Giants

III Giants

IV Subgiants

V Dwarfs

VI Subdwarfs

VII White Dwarfs

Metallicity

The metallicity of a star is the proportion of its mass which is made up from elements other than hydrogen or helium. The metallicity varies mainly between the generations of stars. The youngest stars known as Population I stars have a higher metallicity because they were formed from products of the supernovae from the older Population II stars. The Population II stars are the oldest observed stars and these have very low metallicities.

Theoretically there should also exist the effectively metal free Population III stars which would be the first stars formed after the Big Bang. However there have been no direct observations of them as of yet.

The presence of metals produces absorption lines in the observed spectrum. Note that the metallicity does not vary significantly over the life time of a star, and so it may be used to produce an estimate of the age of the star by assigning it to either the young, metal-rich Population I stars or the older, metal-poor Population II stars.

Stellar Evolution

Stars on the main sequence fuse hydrogen nuclei to produce helium nuclei in the the core by the proton-proton chain, this provides the pressure to resist the gravitational attraction which would cause the star to collapse in on itself if unopposed[3]. Eventually the stars deplete all the hydrogen fuel in the core and the fusion stops, this results in the core contracting and the temperature increasing, this increased temperature then makes it possible to fuse helium nuclei together to form carbon nuclei in the triple alpha process, and the stars become red giants.

This increase in temperature and luminosity means that the stars drift off the main sequence on HR diagrams as they become red giants. This turning point can be modelled and used to estimate the age of star clusters, since it is known how long it takes a star of a particular spectral class to reach the end of its main sequence lifetime.

The Magnitude System

The flux of an object is the amount of radiation received per unit area per unit time. The magnitude system is used to quantify the flux, relative to a standard star, for the purposes of comparison[1]. The scale is logarithmic to the base 10, because the response of the human eye is logarithmic. The equation for the apparent magnitude of the star (the magnitude independent of distance) is given in Equation (5).

$$m - m_0 = 2.5 \log_{10}(F_0/F) \tag{5}$$

Where m is the apparent magnitude, m_0 is the magnitude of the standard star, F is the flux of the observed star, and F_0 is the flux of the standard star. Note that this equation means that brighter starts have lower numerical apparent magnitudes.

The star Vega is used as the standard star and is defined to have a magnitude of $m_0 = 0$, since the flux is well-measured at many wavelengths.

The absolute magnitude takes in to account the distance to the star. The equation for the absolute magnitude is given in Equation (6).

$$M = m - 5 \log_{10}(D_{\mathrm{pc}}) + 5 \tag{6}$$

Where M is the absolute magnitude, m is the apparent magnitude and D_{pc} is the distance to the object in parsecs.

The absolute magnitude is defined as the magnitude that the object would have if it were at a distance of ten parsecs, and so this removes the effect of variable distance and allows for the direct comparison of the luminosity of different stars.

Magnitudes are measured for a broad range of wavelengths, the difference in magnitudes of an object, between wavelength filters, is known as the colour index.

Note that the magnitude axis is plotted from positive to negative on a colour-magnitude diagram since negative magnitude values relate to a higher luminosity than positive ones.

The magnitude relates to the luminosity of the star (the more negative the magnitude is, the brighter the star is), whilst the colour relates to the temperature of the star as described previously, which defines the spectral class of the star (from O, B, A, F , G, K and M, in order of temperature from hot to cool).

The use of colour-magnitude diagrams can also produce an estimate for the age of a star cluster by the fitting of isochrones from stellar evolution models. This could then be compared with the estimated age from the metallicity.

METHOD

Observation

To obtain enough light through the spectrometer, bright stars and other objects were chosen as targets, so that short integration times could be used and the problems of tracking minimised. In addition to the spectra from the target stars, the spectra from arc lamps was obtained to provide a scale for the observed wavelengths

and the spectrum of a class A star was also necessary to provide a scale for the flux measurements, in this investigation Sirius was used as the reference.

The astronomical objects chosen for observation were Sirius, Betelgeuse, the Moon, and Mars. A spectrum of the daytime sky was also taken for comparison.

Analysis

The data was analysed using the *IRAF* software package.

The arc lamps were used to calibrate the wavelength scale of the CCD output. The known lines were measured and assigned their wavelengths so the scale is calibrated correctly.

The flux scale was calibrated from the CCD counts by observing Sirius, as it has few absorption lines and a known temperature, and then fitting a blackbody distribution at the known temperature to the CCD count distribution, so the flux at each point could be assigned.

The contribution from the sky background was subtracted using *IRAF*, since the stars do not completely fill the field of view and so there is a large contribution from the sky in each spectra which can be accounted for and removed.

To produce the final astronomical spectra, four calibration images were necessary:

Flatfield image: The flatfield image (also known as a "sky flat" when of a blank sky or a "dome flat" when of a uniformly illuminated panel) is an image taken of a source of uniform illumination. This is then used to adjust for the differences between the gain in pixels in the CCD and so normalise the corrected image as they are divided by it. In this case it is advantageous to use the most luminous source possible that does not saturate the CCD pixels, so the relative difference is greatest.

Dark Frame: This is an image of a completely dark area (i.e. with the shutter closed) and it is subtracted from the image to compensate for the CCD counts produced by thermal effects.

Bias Frame: The bias frame is an image taken with no exposure time, and is subtracted from the image to compensate for the effects of noise produced by the electronics of the CCD.

Sky Background: This is an image of an empty sky, taken at the same time as the astronomical images, and is subtracted from the images to correct for the effects of atmospheric light diffusion (including artificial light pollution).

Note that the telescope automatically produces the dark frame and bias frame to account for the electronic and thermal effects of the CCD. The exposure times were selected from trial and error, to obtain enough light without saturating the CCD.

The continuum spectrum was only measured within the visible spectrum, however this may be used to fit a blackbody distribution to the spectrum as it would be without the presence of absorption peaks. The temperature could be estimated by fitting a blackbody distribution to the spectra, or more simply by using Wien's Law, given in Equation (2), with the value of the peak emitted wavelength.

The spectral lines were also identified,the temperature can also be estimated from the strength of the Balmer series (as strong Balmer peaks indicate a class A star), and this can be checked with the estimated surface temperature from Wien's Law.

The metallicity of the stars could also be estimated from the relative abundance of the metals, and the relative radial velocity of the stars could be estimated from the Doppler shift of the absorption peaks compared to known positions. However both of these calculations require very high-resolution spectra, and so were not possible in this investigation.

RESULTS

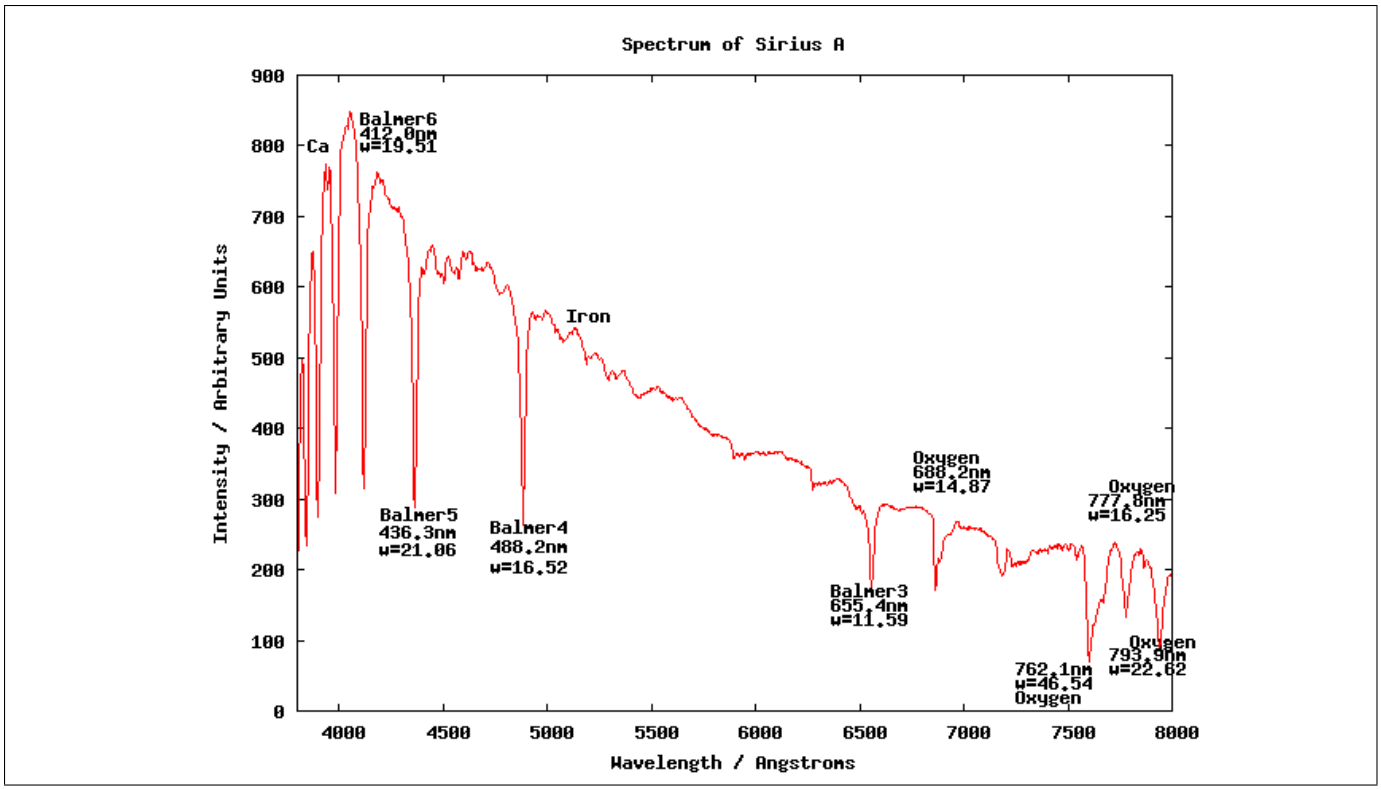

FIG. 2: The spectrum produced for Sirius A.

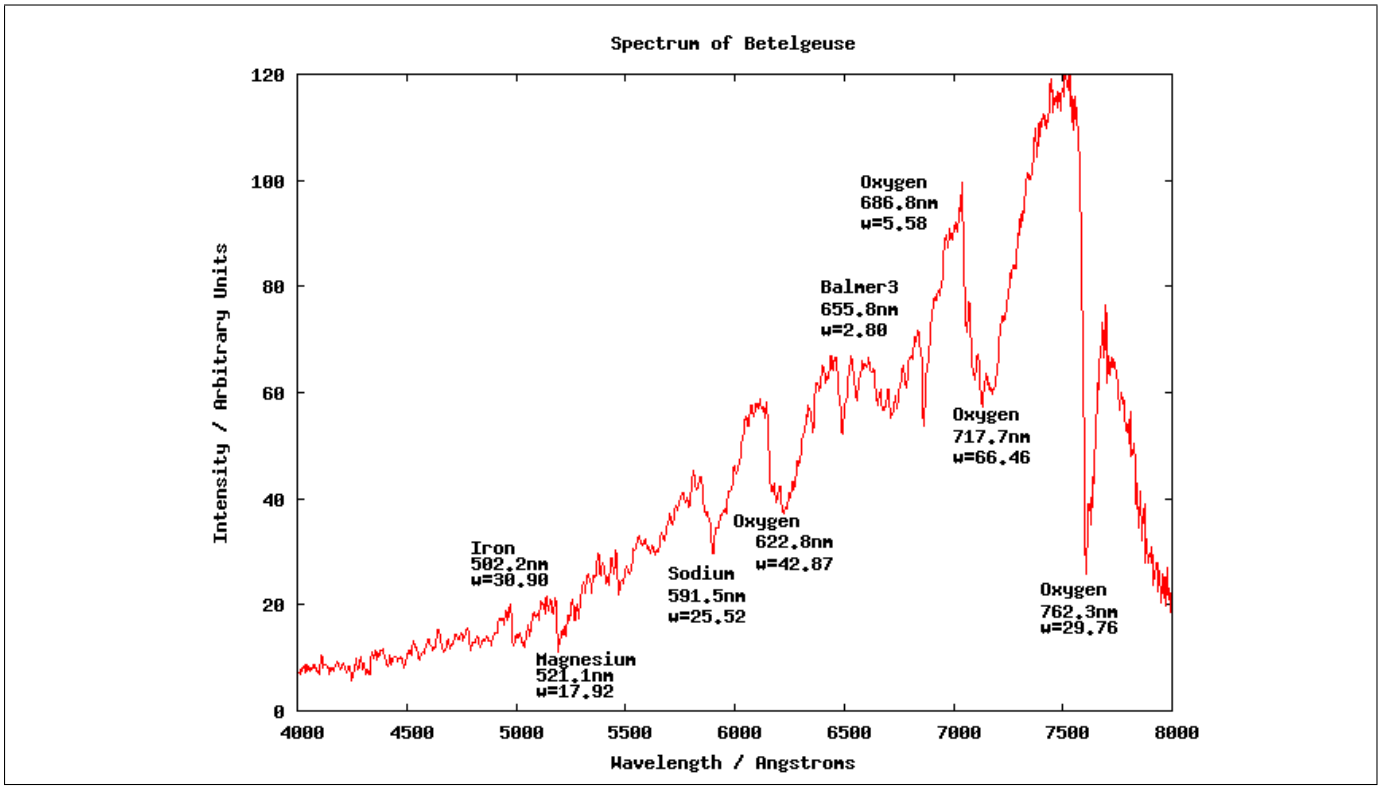

FIG. 3: The spectrum produced for Betelgeuse.

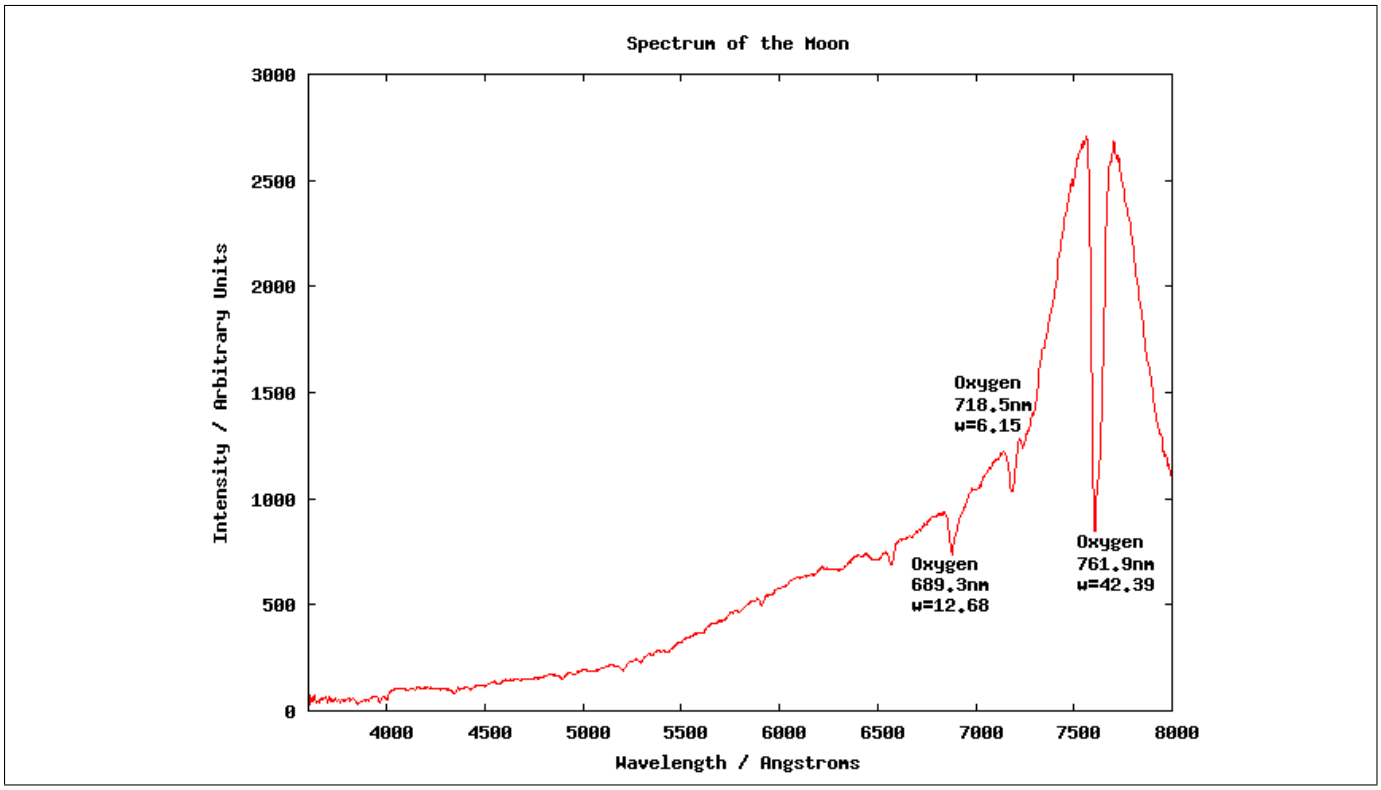

FIG. 4: The spectrum produced for the Moon.

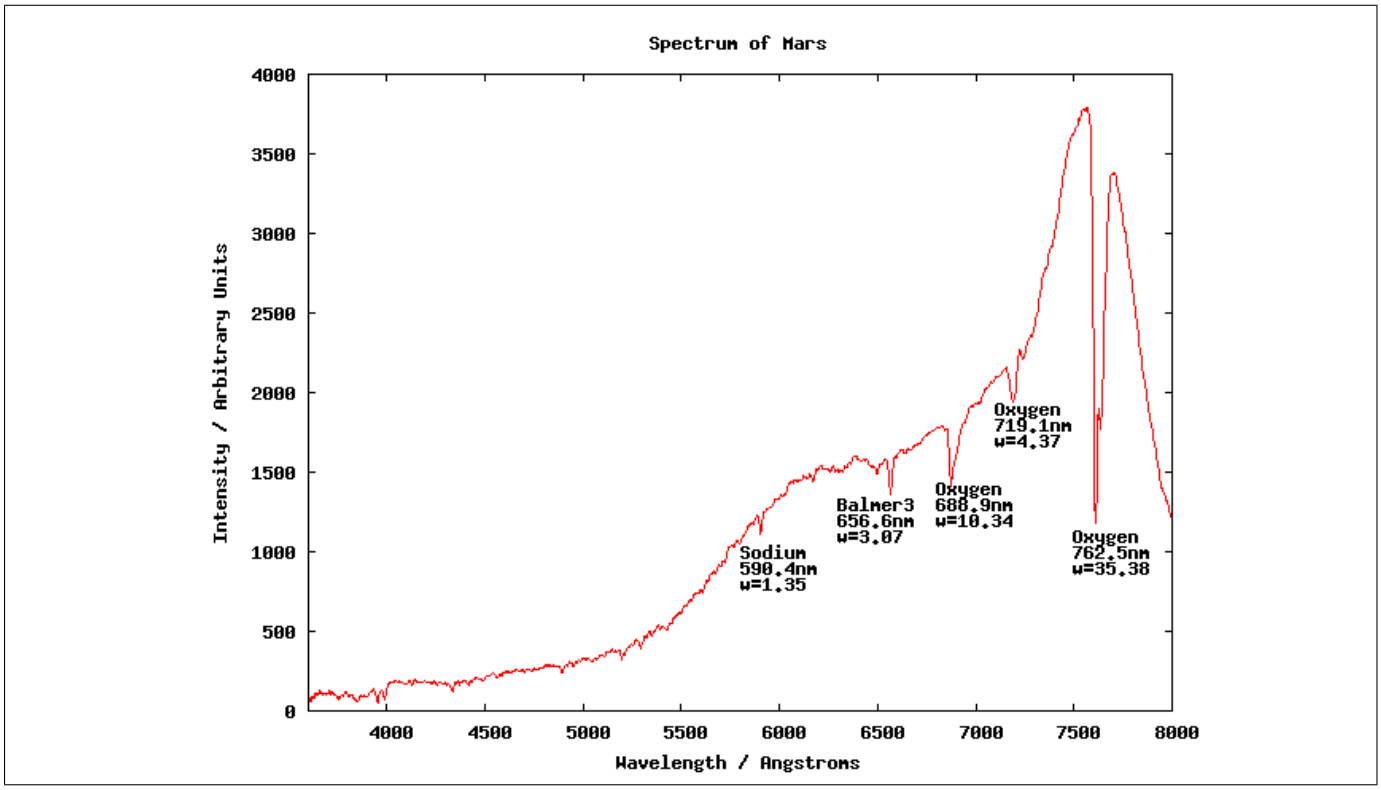

FIG. 5: The spectrum produced for Mars.

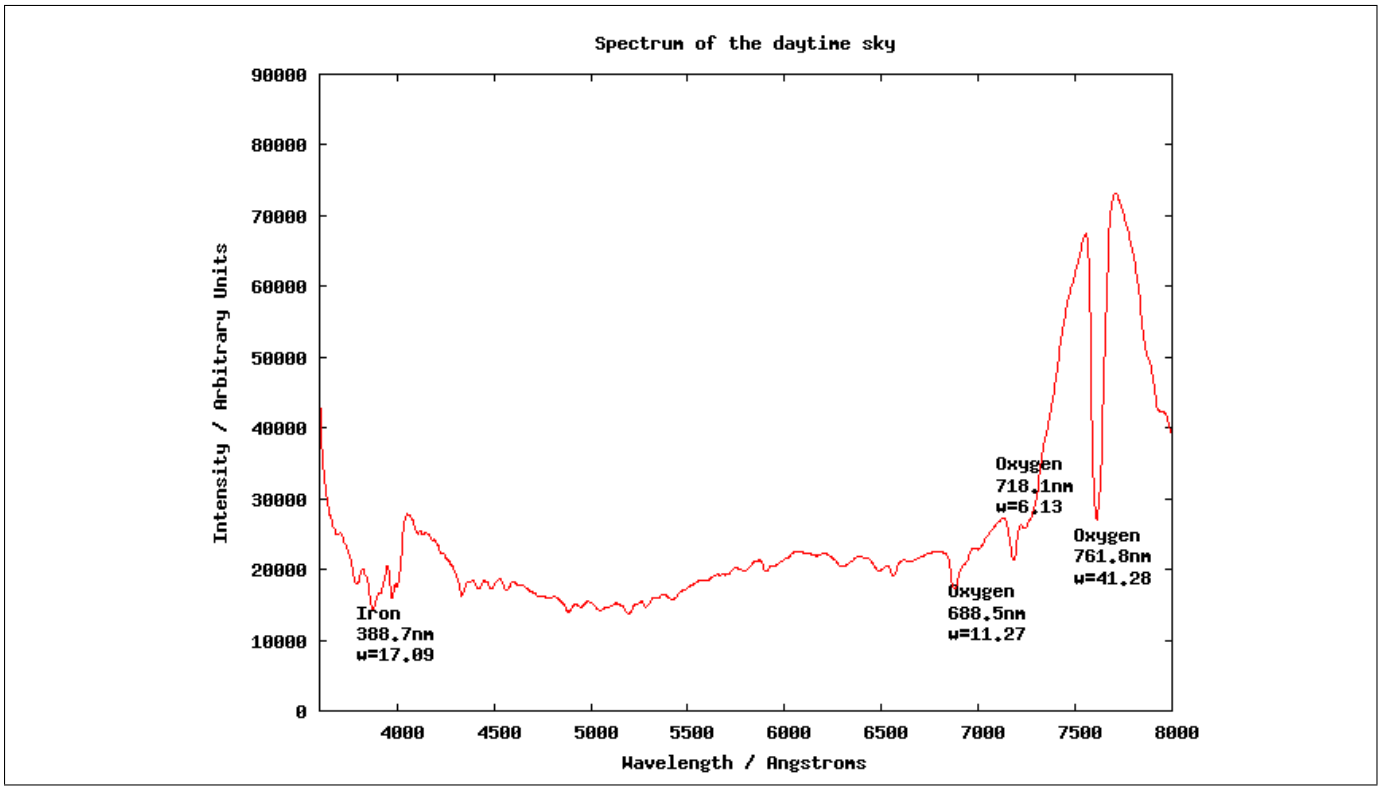

FIG. 6: The spectrum produced for the daytime sky.

DISCUSSION

The spectral lines in the graphs were identified from the known Fraunhofer lines[4], the errors in the peak wavelengths varied up to 20 angstroms compared to the CHIANTI database[5] for known emission lines in laboratory conditions.

Errors in the equivalent widths can be estimated by assuming that the equivalent widths of the same oxygen absorption lines were mostly constant, and so using the spectra from the Moon and Mars the error in the equivalent width measurements was approximately 7 units.

The objects' colours are dictated by where the majority of emission lies, and so Sirius appears white due to having a large amount of radiation across the whole visible spectrum. Whereas Mars and Betelgeuse appear red due to peaking in the red wavelength area.

The oxygen peaks on the right of the spectra are the result of telluric contamination, as oxygen in the Earth's atmosphere absorbs these wavelengths, and are not part of the stars absorption pattern. At near-UV wavelengths the Earth's atmosphere absorbs almost all radiation, and so the spectra are truncated around 4000 angstroms.

The Moon and the daytime sky appear red on the spectra, this is likely due to an error in the spectra obtained, especially as the light source was poor due to the crescent moon in the case of the moon's spectrum. However, the response of the eye is also non-uniform, with a greater response in the green and yellow wavelengths, so this may also explain the spectra. The daytime sky however, has no such effect, and should appear blue as the blue light is scattered more in the atmosphere. The exact cause of the anomalies in these spectra is unknown, however it may be related to the atmospheric absorption at low wavelengths affecting the flux calibration of the solar spectrum (as the signal to noise ratio decreases with more absorption).

Note that the Balmer peak which appears in the Mars spectrum is not a result of the Martian atmosphere itself, but due to the fact it is reflecting the Sun's light. This is the same cause as the metallic lines in the daytime spectrum.

Sirius contains strong Balmer peaks as it is a class A main sequence star, and so contains a lot of Hydrogen in in the outer shells of the star, at the right temperature to produce the Balmer peaks. Betelgeuse does not have such strong Balmer peaks as it is a class M star (a red giant), and so does not have so much Hydrogen in the shells of the star.

Some metallic peaks are visible on the Sirius spectrum, as it is a Population 1, class A star and so contains metals from the previous supernovae it was formed from and also iron forming in the core. However, the resolution of the spectrum is not high enough to produce a reasonable estimation of the metallicity. The same constraint also prevents an estimation of the radial velocity from the Doppler shift of the lines.

Calculation of effective temperatures

From the position of the peak emission and Wien's law (Equation (2)) the effective surface temperatures in Table I was produced.

TABLE I. Estimates of the effective surface temperatures for objects, calculated from Wien's law

Star	$\lambda_{\max}/\mathring{A} \pm 100\mathring{A}$	T/K $\pm 200K$	Accepted temperature[1] / K
Sirius	4053	7149	9940
Mars	7600	3813	5800 (Sun)
Betelgeuse	7500	3838	3500
Moon	7591	3817	5800 (Sun)
Daytime Sky	7694	3766	5800 (Sun)

The calculation for Sirius was not consistent with the accepted value. This may have been due to the Earth's atmosphere absorbing low wavelengths which alters the spectrum, the strong absorption peaks altering the position of the peak wavelength or reddening effects from interstellar dust. The estimated temperature for Betelgeuse was also not consistent with the accepted result, however it was much closer. The errors were calculated from the error in determining the peak wavelength (note this is greater than the error in the individual wavelengths due to the presence of absorption lines altering the structure near the peak), and assuming there was no error in Wien's constant.

The other objects temperatures were not consistent with the Sun's temperature, however this is not surprising as the effects of the Earth's atmosphere scattering the sunlight and the Martian atmosphere would alter the spectra significantly.

CONCLUSION

The spectra of Sirius, Betelgeuse, Mars, the Moon and the daytime sky were taken. The effective temperatures of the objects were estimated, assuming they fit a model of blackbody radiation, using Wien's law. Betelgeuse's temperature was estimate to be 3838 ± 200K which is not consistent with the accepted value of 3500K[1], Sirius's temperature was estimated to be 7149 ± 200K which is not consistent with the accepted value of 9940K. The estimated temperatures for the other objects was also not consistent with the temperature of the Sun, however this is not surprising, as the reflection and atmospheric effects will alter the spectrum.

Possible extensions

To extend the experiment a polarizer could be fit to the spectrometer to investigate the Zeeman effect. The Zeeman effect is analogous to the Stark effect but is caused by external magnetic fields which then produce the change and splitting in energy levels. This produces polarised light which could be investigated.

Higher resolution spectra could also be obtained so that the radial velocity could be estimated from the Doppler shift in the absorption lines and the metallicity of the stars could also be calculated. However, this would require long exposure times and so would also require accurate tracking. Estimates for the age of the stars from the population type (determined by the metallicity) could then be compared to estimates of the age of the stars from Colour-Magnitude diagrams fitted with isochrones from models of stellar evolution to verify their accuracy.

A larger range of wavelengths could also be studied, however no one telescope can observe all wavelengths so this would require more equipment. The Earth's atmosphere also absorbs radiation at ultraviolet and infra-red wavelengths, however the use of radio waves could be effective (although these interact with the ionosphere at some wavelengths).

[1] I. Morison, in *Introduction to Astronomy and Cosmology* (Wiley, Chichester, UK, 2008) p. 26, ISBN 978-0-470-03333-3

[2] L. Harra and K. Mason, in *Space Science* (Imperial College Press, London, 2004) p. 251, ISBN 1-86094-346-2

[3] M. Inglis, *Astrophysics is easy!* (Springer, 2007) ISBN 978-1-85233-890-9

[4] F. Jenkins and H. White, in *Fundamentals of Optics* (McGraw-Hill, 1981) p. 18, 4th ed., ISBN 0072561912

[5] Dere *et al.*, A&As **125**, 149 (1997)